

Accepted Manuscript

Synthesis of different heterocycles-linked chalcone conjugates as cytotoxic agents and tubulin polymerization inhibitors

Nagula Shankaraiah, Shalini Nekkanti, Uma Rani Brahma, Niggula Praveen Kumar, Namrata Deshpande, Daasi Prasanna, Kishna Ram Senwar, Uppu Jaya Lakshmi

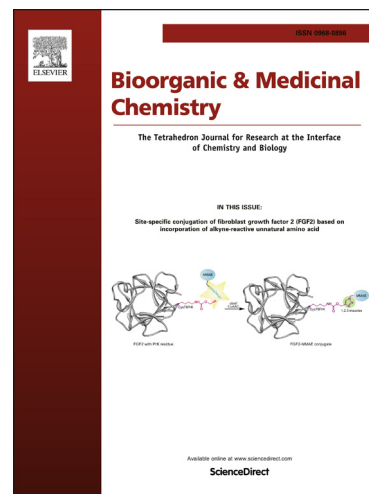
PII: S0968-0896(17)31242-7
DOI: <http://dx.doi.org/10.1016/j.bmc.2017.07.031>
Reference: BMC 13868

To appear in: *Bioorganic & Medicinal Chemistry*

Received Date: 15 June 2017
Revised Date: 13 July 2017
Accepted Date: 15 July 2017

Please cite this article as: Shankaraiah, N., Nekkanti, S., Brahma, U.R., Praveen Kumar, N., Deshpande, N., Prasanna, D., Senwar, K.R., Lakshmi, U.J., Synthesis of different heterocycles-linked chalcone conjugates as cytotoxic agents and tubulin polymerization inhibitors, *Bioorganic & Medicinal Chemistry* (2017), doi: <http://dx.doi.org/10.1016/j.bmc.2017.07.031>

This is a PDF file of an unedited manuscript that has been accepted for publication. As a service to our customers we are providing this early version of the manuscript. The manuscript will undergo copyediting, typesetting, and review of the resulting proof before it is published in its final form. Please note that during the production process errors may be discovered which could affect the content, and all legal disclaimers that apply to the journal pertain.



Synthesis of different heterocycles-linked chalcone conjugates as cytotoxic agents and tubulin polymerization inhibitors

Nagula Shankaraiah,^{a*} Shalini Nekkanti,^a Uma Rani Brahma,^b Niggula Praveen Kumar,^a Namrata Deshpande,^a Daasi Prasanna,^a Kishna Ram Senwar,^a Uppu Jaya Lakshmi^b

^aDepartment of Medicinal Chemistry, National Institute of Pharmaceutical Education and Research (NIPER), Hyderabad-500 037, India

^bDepartment of Pharmacology & Toxicology, National Institute of Pharmaceutical Education and Research (NIPER), Hyderabad-500 037, India

*Corresponding author. Tel.: (+91) 040 23073740; Fax: (+91) 040 23073751; E-mail: shankar@niperhyd.ac.in; shankarnbs@gmail.com

Abstract: A series of new heterocycles-linked chalcone conjugates has been designed and synthesized by varying different alkane spacers. These conjugates were tested for their *in vitro* cytotoxic potential against a panel of selected human cancer cell lines namely, lung (A549 and NCI-H460), prostate (DU-145 and PC-3), colon (HCT-15 and HCT-116), and brain (U-87 glioblastoma) by MTT assay. Notably, among all the tested compounds, **4a** exhibited potent cytotoxicity on NCI-H460 (lung cancer) cells with IC₅₀ of 1.48 ± 0.19 μM. The compound **4a** showed significant inhibition of tubulin polymerization and disruption of the formation of microtubules (IC₅₀ of 9.66 ± 0.06 μM). Moreover, phase contrast microscopy and DAPI staining studies indicated that compound **4a** can induce apoptosis in NCI-H460 cells. Further, the flow-cytometry analysis revealed that compound **4a** arrests NCI-H460 cells in the G2/M phase of the cell cycle. In addition, molecular docking studies of the most active compounds **4a** and **4b** selectively bind into colchicine site of the tubulin, revealed the possible mode of interaction by these new conjugates.

Keywords: Heterocycles, anticancer activity, chalcones, aldol condensation, tubulin polymerization inhibitor, molecular modeling.

1. Introduction

Tubulin is an α,β -heterodimeric protein that forms the cytoskeletal framework of microtubules.¹ It is one of the most active molecular targets of numerous anticancer ligands that cause cell cycle arrest at the G2/M phase by interfering with the microtubule polymerization/depolymerization process.^{2,3} Many clinically used natural product anticancer agents such as colchicines (**A**, **Figure 1**), MDL-27048, taxanes, combretastatin A-4 (**B**), podophyllotoxin and vinca alkaloids are tubulin-binding agents.⁴ Antimitotic agents generally interact with tubulin at three known binding sites namely, the colchicine, the vinca alkaloid and the paclitaxel binding sites. Agents that target the colchicine site (e.g., colchicines, combretastatin A-4 and podophyllotoxin)⁵ or the vinca alkaloid site (e.g., vinblastine)⁶ are known as microtubule destabilizing agents. On the other hand, agents that bind to the paclitaxel site (e.g., paclitaxel)⁷ are referred to as microtubule-stabilizing agents. As microtubules play a vital role in several cellular functions such as the formation of the mitotic spindle, cytoplasmic organelle movement, maintaining cell shape, intracellular transport and cell replication, interfering with microtubule dynamics lead to severe side effects.⁸⁻¹⁰ Therefore, it is essential to develop new tubulin-binding agents and antimitotic agents with novel modes of action to overcome side effects as well as drug resistance.

Chalcones (1,3-diaryl-2-propen-1-ones) are precursors of flavonoids and isoflavonoids that possess a wide range of biological activities such as anticancer, anti-diabetic, anti-hypertensive, anti-viral, anti-inflammatory, anti-tuberculosis, anti-oxidant, anti-leishmanial, anti-filarial, anti-malarial, anti-bacterial and anti-fungal activities.¹¹⁻¹⁴ The biological activities of chalcones are largely attributed to the presence of α,β -unsaturated ketone functionality, as removal of this group makes them inactive. The extensive exploration of chalcones can be attributed to their ease of synthesis, relatively simpler chemical architecture, being precursors for important synthetic manipulations and promising biological activities. Naturally occurring chalcones and their synthetic analogs displayed significant cytotoxic activity against various cancer cells.¹⁵ One of the most widely proposed anticancer mechanisms of chalcones is the prevention of tubulin polymerization by binding to the colchicine-binding site.¹⁶⁻¹⁸ Due to their promising anti-cancer activities, considerable efforts have been dedicated to discovering new potential chalcone-based drug candidates during the last decade. A majority of these naturally occurring anti-cancer compounds are substituted with electron donating hydroxy and/or methoxy

groups at various positions around the chalcone scaffold.^{19,20} In order to ascertain more advanced structure–activity relationships (SARs) of chalcones, it is of great importance to synthesize new compounds with more diverse substitutions patterns.

In continuation of our earlier efforts in the field of anti-cancer drug discovery,^{21–25} herein, we report the synthesis of a series of novel heterocycles-linked chalcone conjugates (**C**, **Figure 1**) with diverse substitutions and evaluated for their *in vitro* cytotoxic activity on selected human cancer cell lines.

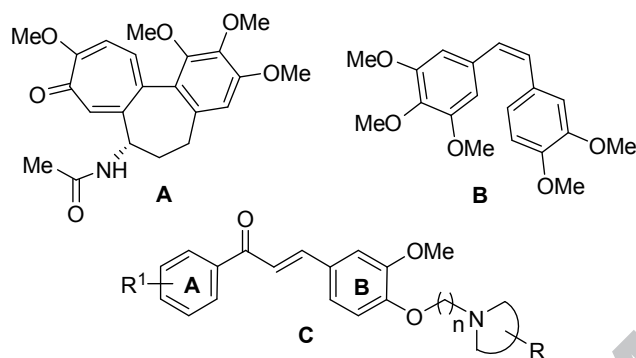


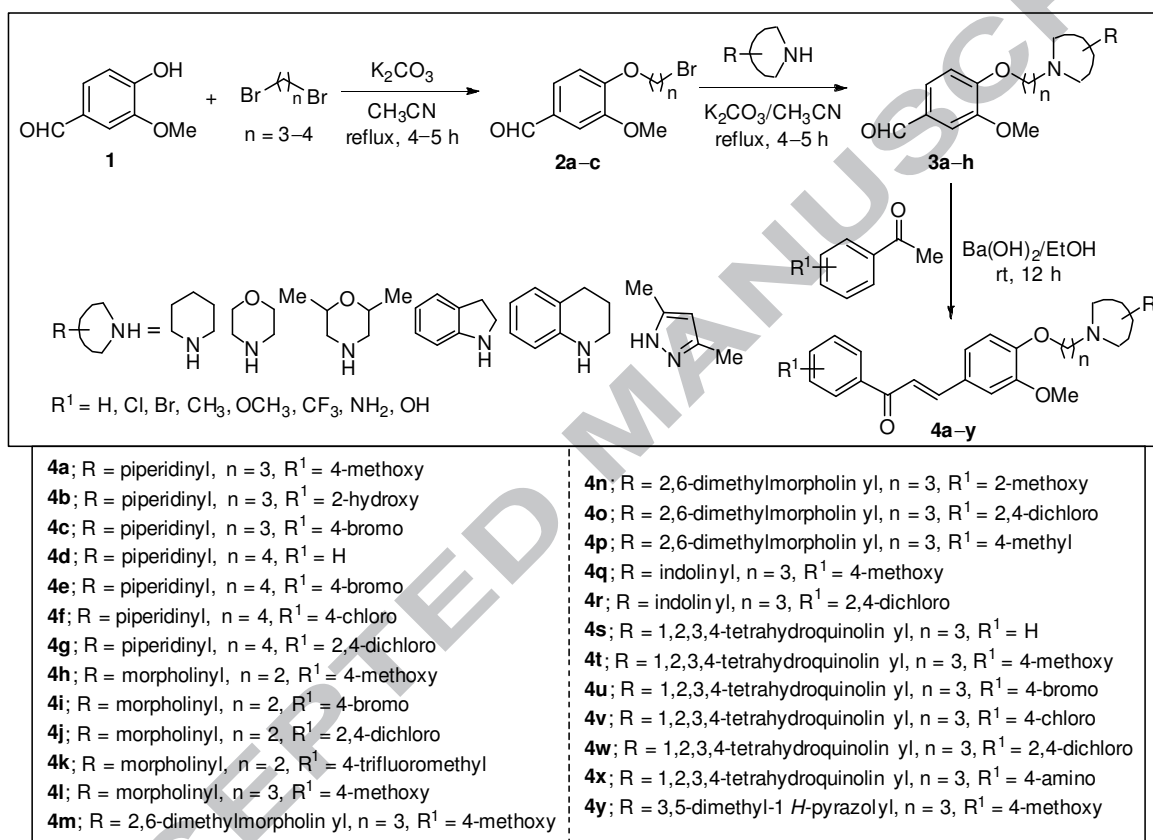
Fig. 1. The structures of colchicine (**A**), combretastatin A-4 (**B**), and heterocycles-linked new chalcone conjugates **4a–y**.

2. Results and discussion

2.1. Chemistry

Two core structural components (i) an aldehyde, and (ii) a ketone are required for achieving the target chalcone conjugates **4a–y**. The synthetic route for the preparation of the heterocycles-linked chalcone conjugates **4a–y** was outlined in **Scheme 1**. Initially, the etherification of vanillin (**1**) was carried out with dibromo alkane spacers of varying lengths ($n = 2,3,4$), in the presence of K_2CO_3 as the base to give the intermediates **2a–c**. Next, various nitrogen containing heterocycles were tethered to the alkane spacer of **2** by refluxing in acetonitrile in the presence of K_2CO_3 , to afford the aldehyde intermediates **3a–h** in quantitative yields. Finally, aldol condensation reaction was performed between intermediates **3a–h** and a variety of substituted acetophenones by using $Ba(OH)_2$ as the base to furnish the chalcone derivatives **4a–y** in good yields. All the newly synthesized compounds were characterized by HRMS, 1H and ^{13}C NMR spectroscopy.

Almost similar pattern was observed in ^1H and ^{13}C NMR spectra of all the final synthesized compounds of this series. The double bond of the chalcone moiety was in the *trans*-configuration as denoted by the coupling constant (J) values of 15–16 Hz. In the ^{13}C NMR spectrum, the characteristic peaks corresponding to the chalcone moiety were observed: the carbonyl carbon appeared in the range δ 183–192 whereas the aromatic carbons along with the olefinic carbons appeared in the range of δ 163–104. The HRMS (ESI) of all the compounds showed an $[\text{M} + \text{H}]^+$ peak equivalent to their molecular formulae.



Scheme 1. Synthesis of different heterocycles-linked new chalcone conjugates **4a–y**.

2.2. Biological evaluation

2.2.1. *In vitro* cell growth inhibitory activity

The new chalcone conjugates **4a–y** were evaluated for their *in vitro* antiproliferative activity against a panel of seven human cancer cell lines namely, lung (A549 and NCI-H460), prostate (DU-145 and PC-3), colon (HCT-15 and HCT-116) and brain (U-87 glioblastoma) by using 3-(4,5-dimethylthiazol-2-yl)-2,5-diphenyltetrazolium bromide (MTT) assay. Concentration-

response course analysis was carried out to establish the drug concentration required to inhibit the growth of cancer cells by 50% (IC_{50}) after incubation for 48 h. Combretastatin A-4 (CA-4) was used as the reference standard and the screening results were summarized in **Table 1**.

It is noticeable from the initial screening that the hybrids **4a**, **4b**, **4l** and **4y** displayed a broad range of activities against all the tested human cancer cell lines with IC_{50} values ranging from $1.48 \pm 0.19 \mu\text{M}$ to $10.98 \pm 0.81 \mu\text{M}$. Among them, the most potent compound was **4a** with IC_{50} values of 1.48 ± 0.19 and $1.73 \pm 0.16 \mu\text{M}$ against NCI-H460 and HCT-116 cell lines, respectively. Moreover, the compound **4a** was also found to be active against all the tested cancer cell lines with IC_{50} values less than $10 \mu\text{M}$. Interestingly, the compound **4b** was found to be active in all the seven cancer cell lines with IC_{50} values in the range of 1.63 ± 0.15 to $3.24 \pm 1.2 \mu\text{M}$. The compounds **4b** and **4y** showed potent cytotoxic activity on the HCT-15 cell line, with IC_{50} values less than $5 \mu\text{M}$, which was significant compared to the activity of CA-4 (IC_{50} $8.87 \pm 0.88 \mu\text{M}$). Except for **4l**, **4m**, **4n**, **4p** and **4y**, all other chalcone conjugates were found to be inactive on the HCT-116 cell line. These five compounds **4l**, **4m**, **4n**, **4p** and **4y** were also effective against the U-87 and A549 cell lines. It was also observed that, in DU-145 cell line, the compounds **4l**, **4m** and **4n** displayed potent cytotoxicities with IC_{50} values of 2.02 ± 0.14 , 3.27 ± 1.16 and $3.87 \pm 1.0 \mu\text{M}$, respectively. In the PC-3 cell line, except **4b** (IC_{50} $1.95 \pm 0.02 \mu\text{M}$), none of the compounds showed better activity than CA-4 (IC_{50} $3.53 \pm 1.1 \mu\text{M}$). The compounds **4r-w** were found to be inactive against all the cell lines, with IC_{50} values greater than $15 \mu\text{M}$.

Based on the *in vitro* cytotoxic activities, the structural activity relationships (SARs) of the chalcones **4a-y** have been proposed. In order to comprehend the SARs, we varied the substitutions on both the A and B rings, the length of the linkers as well as the nitrogen heterocycles in these conjugates. It could be easily observed from the *in vitro* cytotoxicity data that the conjugates with piperidine (**4a** and **4b**) and morpholine (**4l**) linked to the B ring elevated the biological response, compared to those with other nitrogen heterocycles. The presence of larger nitrogen heterocycles such as indoline and tetrahydroquinoline (**4q-x**) completely abolished the cytotoxic activity. The effect of substitution on ring A is interesting in the light of the results of the SAR study, which demonstrates that the presence of electron-donating groups such as 2-hydroxy and 4-methoxy (**4a**, **4b**, **4l**, **4m** and **4y**) is favorable for activity, in contrast, electron withdrawing groups such as 4-chloro, 4-bromo (**4c**, **4e-g**, etc) resulted in significant loss

of activity. The importance of linker length on cytotoxic activity is demonstrated by the fact that analogues with the linker length of three showed enhanced cytotoxicity than those with linker lengths of two or four. Based on the promising cytotoxic activity, the most active compounds **4a** from this series was taken-up for detailed further studies.

Table 1. Cytotoxic activity (IC₅₀ in μM)^a of heterocycles-linked new chalcone conjugates **4a–y**.

Compound	HCT-15 ^b	NCI-H460 ^c	HCT-116 ^d	U-87 ^e	DU145 ^f	PC-3 ^g	A549 ^h
4a	5.34±0.06	1.48±0.19	1.73±0.16	6.30±0.33	5.08±0.05	9.53±0.01	3.29±0.74
4b	3.24±1.2	1.63±0.15	2.01±1.1	2.87±0.16	2.73±0.14	1.95±0.02	3.13±0.03
4c	>20	8.16±0.98	>20	>20	17.09±0.65	8.93±0.26	16.52±0.96
4d	>20	>20	>20	>20	>20	9.18±0.82	>20
4e	8.97±1.0	>20	>20	4.01±0.09	>20	7.54±1.1	9.06±0.04
4f	8.11±1.0	10.19±0.62	>20	8.01±0.39	7.74±1.01	6.84±0.91	8.99±0.65
4g	>20	16.32±0.35	>20	6.09±1.10	5.73±0.51	7.29±0.22	9.48±0.07
4h	7.54±0.45	9.96±0.18	>20	7.09±0.65	8.74±0.01	9.19±0.39	8.21±0.67
4i	>20	>20	>20	>20	9.74±0.09	8.89±0.98	12.08±0.29
4j	18.23±0.68	>20	19.93±0.62	>20	6.74±0.61	5.12±0.96	>20
4k	>20	>20	>20	>20	>20	6.17±0.26	19.09±0.63
4l	10.98±0.8	9.89±0.9	6.78±0.4	7.12±0.2	2.02±0.14	7.89±0.71	5.36±0.02
4m	8.64±0.6	4.18±0.55	7.87±0.29	5.67±0.08	3.27±1.16	>20	7.42±0.44
4n	6.36±0.1	8.1±0.2	6.48±0.16	5.03±0.09	3.87±1.0	>20	5.32±0.01
4o	>20	>20	>20	>20	>20	8.87±0.19	>20
4p	8.69±0.4	>20	5.45±0.3	4.21±0.45	>20	>20	9.12±0.30
4q	19.92±0.89	>20	>20	15.21±0.82	16.08±0.05	>20	18.68±0.13
4r	>20	>20	19.23±0.86	19.80±0.11	>20	>20	>20
4s	>20	>20	>20	19.75±0.67	>20	>20	>20
4t	>20	>20	>20	18.21±0.92	>20	>20	>20
4u	>20	>20	>20	>20	>20	>20	19.08±0.85
4v	>20	>20	>20	16.21±0.82	18.09±0.65	>20	>20
4w	>20	>20	>20	>20	>20	8.17±0.78	>20
4y	4.03±0.17	8.96±0.18	3.97±1.04	6.93±0.74	5.74±1.0	4.78±0.06	3.70±0.11
CA-4 ⁱ	8.87±0.88	0.048±0.02	9.12±0.52	9.75±0.63	0.28±0.15	3.53±1.1	9.29±0.36

^a 50% inhibitory concentration after 48 h of compound treatment. ^{b,d} Colon cancer cells.

^{c,h} Lung cancer cells. ^e Glioblastoma cancer cells. ^{f,g} Prostate cancer cells. CA-4: Combretastatin A-4, reference compound.

2.2.2. Morphological observations using phase contrast microscope

The induction of the formation of apoptotic bodies has always been an ideal criterion in developing anti-cancer therapeutics. To observe whether the treatment with the compounds could lead to loss of cell viability and induction of apoptosis, NCI-H460 cells were treated with the most active compound **4a**. Cells were observed and photographs were taken with phase contrast microscope. Compound **4a** treated NCI-H460 cells showed cell wall deformation, cell shrinkage and resulted in reduced number of viable cells, whereas these distinctive morphological features were absent in control cells as shown in **Fig. 2**. This indicates that the compound **4a** induces marked morphological changes in NCI-H460 cells.

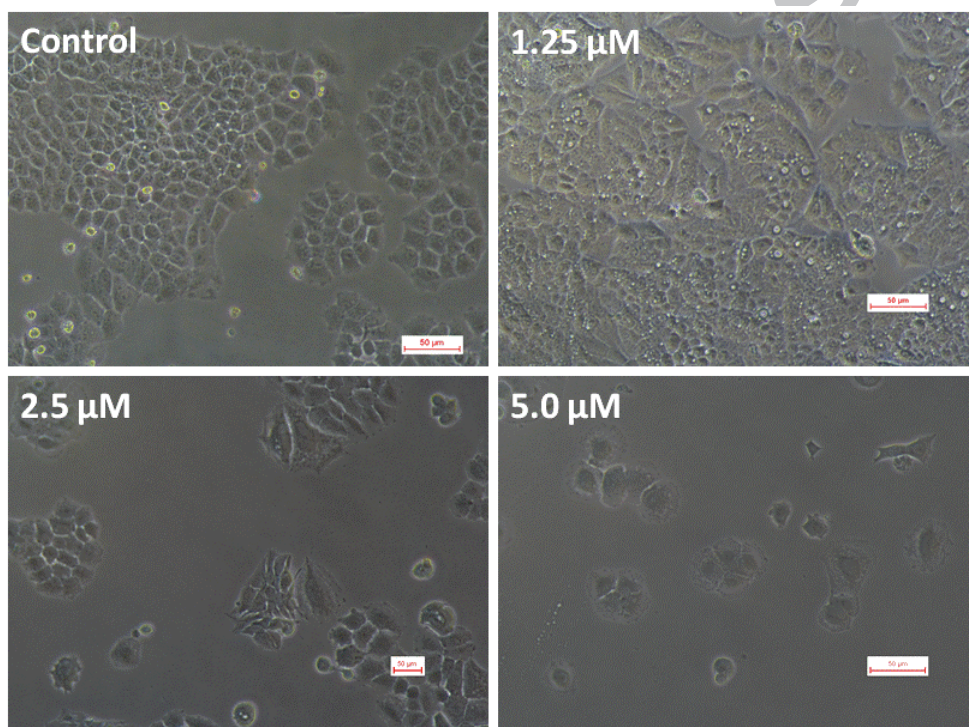


Fig. 2. Effect of the compound **4a** [(a) 0.0 μM ; (b) 1.25 μM ; (c) 2.5 μM ; (d) 5.0 μM] on the morphology and cell viability of NCI-H460 cells.

2.2.3. DAPI nucleic acid staining

DAPI (4',6-diamidino-2-phenylindole) is a fluorescent dye capable of strong binding to A–T rich sequences of DNA and aids in the visualization of chromatin condensation or nuclear damage. It distinguishes live cells from apoptotic cells by staining the characteristic condensed

nuclei of the latter bright blue.²⁶ Therefore, this staining technique was performed to detect the induction of apoptosis by the compound **4a** in NCI-H460 cells. From **Fig. 3**, it was established that the nuclear structure of untreated control cells was intact whereas NCI-H460 cells treated with **4a** displayed condensed, horse-shoe shaped or fragmented nuclei.

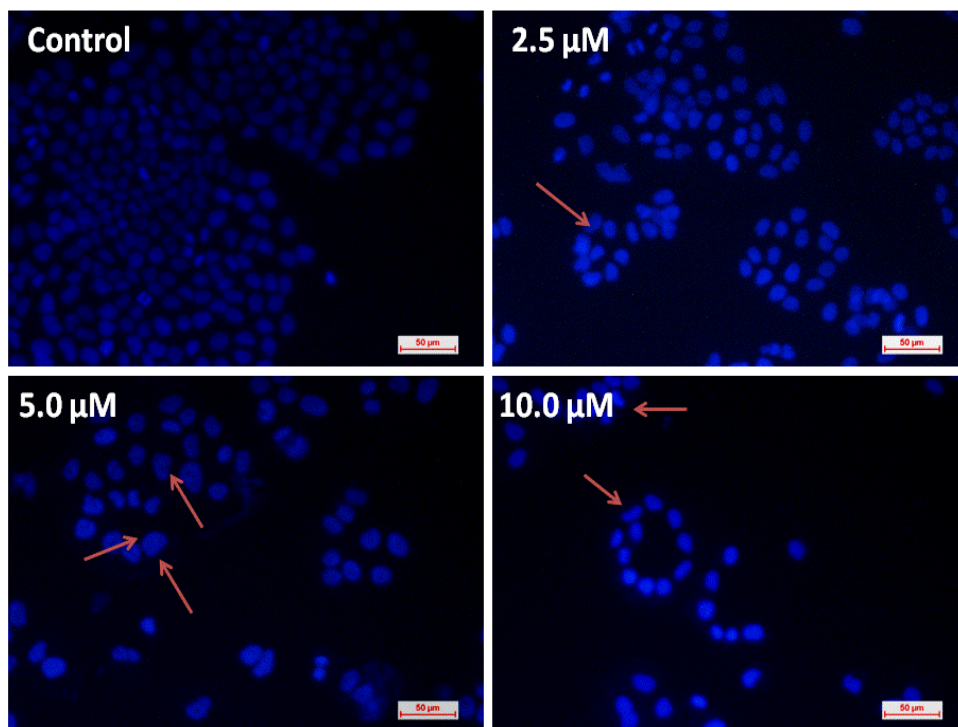


Fig. 3. Nuclear morphology in NCI-H460 cells stained with DAPI. NCI-H460 cells treated with compound **4a** [(a) 0.0 μM ; (b) 2.5 μM ; (c) 5.0 μM ; (d) 10.0 μM] for 24 h were stained with DAPI. The images were captured with a fluorescence microscope.

2.2.4. Generation of Reactive Oxygen Species (ROS)

The generation of ROS is a characteristic feature of many chemotherapeutic agents, thereby initiating oxidative damage to the mitochondrial permeability and membrane potential. Hence, DCFDA staining method²⁷ has been used to assess the generation of intracellular ROS of compound **4a** in NCI-H460 cells. The treatment of compound **4a** for 6 h resulted in enhanced DCFDA fluorescence in a dose-dependent manner, indicating the capability of compounds in accumulating ROS (**Fig. 4**). On the other hand, a decreased fluorescence intensity was observed when NCI-H460 cells were treated with N-acetyl cysteine (NAC) prior to treatment with **4a**, indicating the compound-induced cytotoxicity by ROS generation. Moreover, H_2O_2 treatment of

NCI-H460 cells led to the increased fluorescence when compared to the control due to the generation of free radicals.

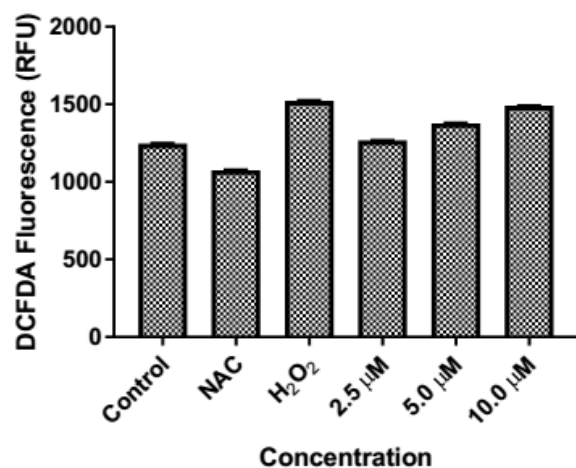
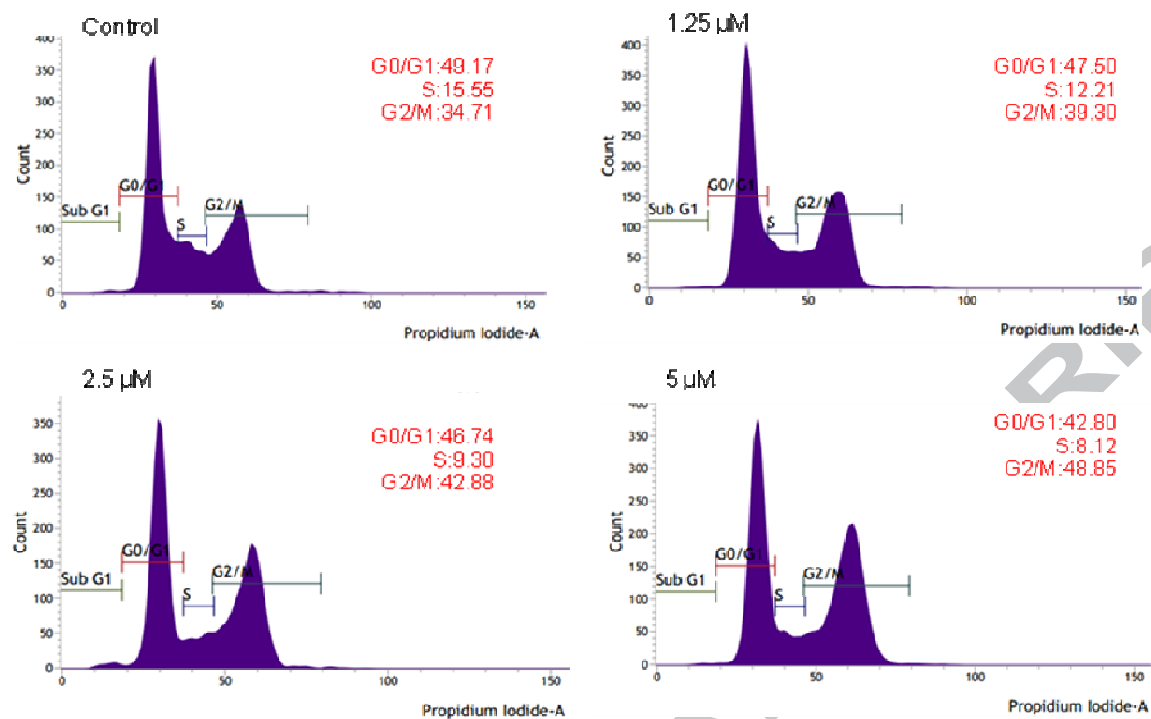


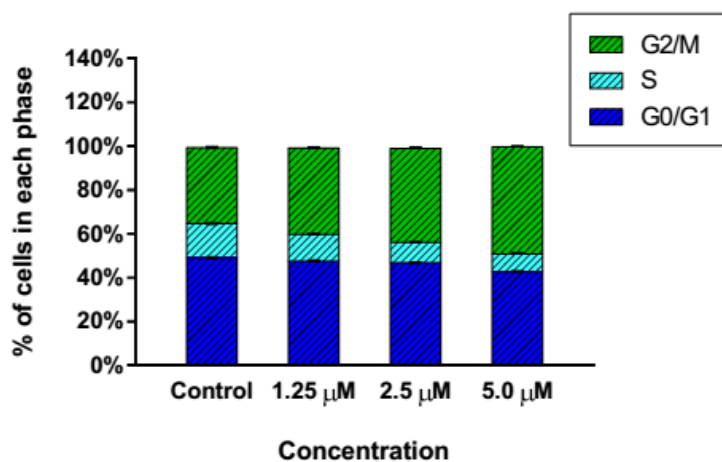
Fig. 4. Effect of compound **4a** on Reactive Oxygen Species' (ROS) levels. Dose-dependent increment of fluorescence was observed compared to control. Each bar represents mean \pm SD from three independent experiments.

2.2.5. Flow-cytometry analysis

Usually, anticancer therapeutics prevent the proliferation of cancer cells by blockade of the cell cycle at a specific checkpoint. From the *in vitro* screening results, it was evident that the compound **4a** showed significant activity against NCI-H460 cells. Hence, it was our interest to figure out whether this cytotoxicity was due to cell cycle arrest, through cell cycle analysis.²⁸ NCI-H460 cells were treated with compounds **4a**, at concentrations of 1.25, 2.5 and 5 μ M for 24 h, stained with propidium iodide and further analyzed by using BD flow cytometry. The results from **Fig. 5** indicated that the NCI-H460 untreated control cells exposed to DMSO showed 34.71% cells in G2/M phase, whereas cells treated with **4a** showed 39.30, 42.88 and 48.85% increase in G2/M population at 1.25, 2.5 and 5 μ M concentrations respectively after 24 h. A simultaneous decreased number of cells in G0/G1 phase were also observed. These results clearly indicated that treatment of NCI-H460 cells with compound **4a** resulted in G2/M phase arrest.



A



B

Fig. 5. Cell cycle analysis of NCI-H460 cancer cells treated with compound **4a** for 24 h. (A) The cell cycle distribution was analysed by using propidium iodide staining method and analysed by flow cytometry (BDc6 accuri). (B) Data of 10,000 cells was collected for each data file. The percentage of the cell population in G0/G1, S and G2/M phase were calculated by using the BDc6accuri software.

2.2.6. Effect on tubulin polymerization

To investigate whether the synthesized compounds can interact with microtubule system in order to elicit antiproliferative activity, the compound **4a** was evaluated for its tubulin polymerization inhibitory activity in a cell-free *in vitro* assay.²⁹ The compound **4a** displayed G2/M cell cycle arrest which is a hallmark of tubulin polymerization. Hence, we investigated the ability of compound **4a** to inhibit tubulin polymerization by monitoring the increase in fluorescence emission at 440 nm (excitation wavelength is 360 nm) for 1 h at 37 °C (**Fig. 6**). In this assay, Combretastatin A-4 (CA-4) and paclitaxel, were used as reference standards at 3 μ M concentration. The compound **4a** were included at final concentrations of 10, 5, 2.5, 1.25, 0.625 μ M respectively. The experiment performed in duplicates. The IC₅₀ value was calculated from the drug concentration required to inhibit 50% of tubulin assembly compared to control. The compound **4a** was found to be a potent inhibitor of tubulin polymerization with an IC₅₀ value of 9.66 ± 0.06 μ M (**Fig. 7**).

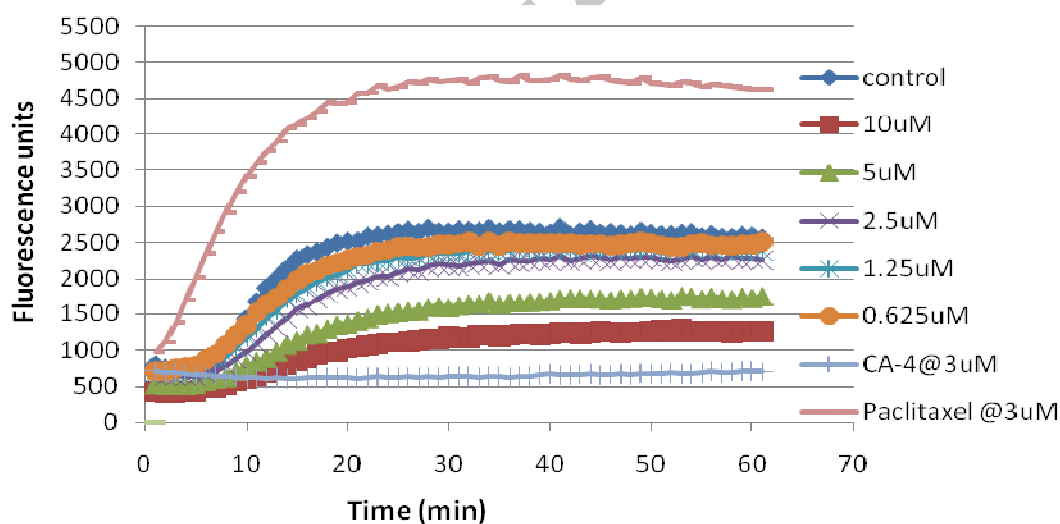


Fig. 6. Effect of compound **4a** on the tubulin polymerization: tubulin polymerization was monitored by the increase in fluorescence at 360 nm (excitation) and 440 nm (emission) for 1 h at 37 °C.

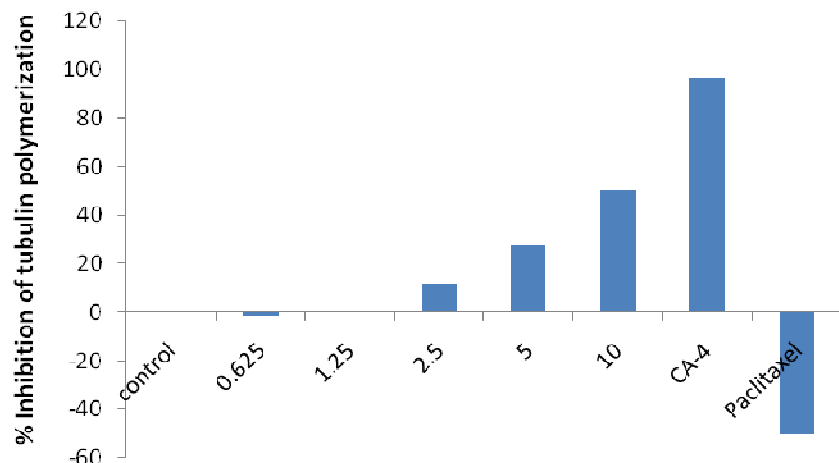


Fig. 7. % Dose-response inhibition of tubulin polymerization by compound **4a** at final concentrations of 10, 5, 2.5, 1.25, 0.625 μM . Combretastatin A-4 (CA-4) and paclitaxel, were used as reference standards at 3 μM concentration.

2.3. Molecular docking

To elucidate the mode of binding with tubulin, the synthesized compounds were docked into the colchicine-binding site of tubulin (PDB ID: 1SA0) located at the interface of the α,β subunits.³⁰ Co-crystallized ligand colchicine was re-docked into tubulin as to validate the docking protocol, with a root mean squared deviation (RMSD) of 0.67 Å. Colchicine interacted strongly with the critical amino acid residues Leu248, Leu255, Asn258 and Lys352 in the colchicine-binding site of tubulin. Therefore, these amino acid residues were very important for the binding of tubulin inhibitors. To confirm the correct binding mode and ensure a geometric fit, compounds **4a** and **4b** were docked into the colchicine-binding site of tubulin (**Fig. 8**).

Compounds **4a** and **4b** exhibited strong hydrophobic interactions with Thr179, Ala316, Lys254 and Met259, as well as critical amino acid residues including Leu248, Leu255, Asn258 and Lys352. We can clearly see that the hydrophobic pockets of colchicine binding site are occupied by A ring and the carbonyl group of the α,β -unsaturated ketone moiety. The ring B and the linker region of molecules extend into the interface between the α - and β -chains which are surrounded by Gln176, Ser178, Tyr210 and Pro255 of the α -subunit and Asp229, Met325 and Val355 of the β -subunit. More importantly, the protonated nitrogen of piperidine formed hydrogen-bonding with the side chain of Asp 329 in both compounds. Moreover, the oxygen atom of the α,β -unsaturated carbonyl system formed a hydrogen-bonding with the side chain of Asn101 (N-

optimal linker length was three; linkers longer or shorter were not efficient in binding to the target site. To gain further insight of our findings, we demonstrated the superimposition of colchicine with the ligands and the corresponding superimposition poses suggest that methoxy phenyl ring of ligands under investigation occupied a similar position with respect to 2-methoxycyclohepta-2,4,6-trien-1-one ring of colchicine and the carbonyl group in **4a** and **4b** superimposes with the amide carbonyl of the colchicines. All these interactions together contribute to the hypothesis that the synthesized compounds exhibit efficient binding into the colchicines binding site on tubulin and thus, the ensuing antimitotic activity.

3. Conclusion

In summary, a series of heterocycles-linked chalcone conjugates were synthesized, and evaluated for their *in vitro* anticancer potential. Interestingly, the compound **4a** showed the most potent antiproliferative activity on the NCI-H460 cell line. Based on the *in vitro* cytotoxic activities, the structure activity relationships (SARs) of the chalcones **4a–y** have been proposed. The presence of piperidine (**4a** and **4b**) and morpholine (**4l**) linked to the ring B together with the presence of electron-donating groups on ring A elevated the biological response. The importance of linker length on cytotoxic activity is demonstrated by the fact that analogues with the linker length of three showed enhanced cytotoxicity than those with linker lengths of two or four. Additionally, **4a** effectively inhibited the polymerization of tubulin through binding at the colchicine binding site. It also induced apoptosis in NCI-H460 cells through the generation of ROS and arresting the G2/M phase of the cell cycle. Overall, the current studies demonstrate that the heterocycles-linked new chalcone conjugate **4a** has the potential to be developed as lead and their further structural modifications may produce promising new cancer therapeutics.

4. Experimental protocols

4.1. Chemistry

All reagents and solvents were obtained from commercial suppliers and were used without further purification. Analytical thin layer chromatography (TLC) was performed on MERCK precoated silica gel 60-F₂₅₄ (0.5 mm) aluminum plates. Visualization of the spots on TLC plates was achieved by UV light. ¹H and ¹³C NMR spectra were recorded on bruker 300 and 500 MHz spectrometers using tetramethyl silane (TMS) as the internal standard. Chemical shifts for ¹H and

^{13}C are reported in parts per million (ppm) downfield from tetra methyl silane. Spin multiplicities are described as s (singlet), bs (broad singlet), d (doublet), dd (double doublet), t (triplet), q (quartet), and m (multiplet). Coupling constant (J) values are reported in hertz (Hz). HRMS were determined with Agilent QTOF mass spectrometer 6540 series instrument.

Wherever required, column chromatography was performed using silica gel (60–120 or 100–200) or neutral alumina.

4.2. General experimental procedure for the synthesis of heterocycles-linked chalcone conjugates **4a–y**

Aldehyde intermediate **3**, acetophenone (1 mmol), and barium hydroxide (1 mmol) were dissolved in EtOH (5 mL). The reaction mixture was stirred for 12 h at room temperature and then evaporated *in vacuo*, water (5 mL) was added and the mixture was neutralized with HCl (1 M, 1.75 mL) and extracted with EtOAc. The organic layer was separated, washed with water, dried, and evaporated *in vacuo*. The residue yielded crude chalcones (**4a–y**) which were purified by column chromatography (Silica gel, 60–120 mesh, 9:1 hexane/ethyl acetate).

4.2.1. (*E*)-3-(3-Methoxy-4-(3-(piperidin-1-yl)propoxy)phenyl)-1-(4-methoxyphenyl)prop-2-en-1-one (**4a**). Yellow liquid, yield 81%; ^1H NMR (500 MHz, CDCl_3): δ 8.03 (d, 2H, $J = 9.0$ Hz), 7.75 (d, 1H, $J = 16.0$ Hz), 7.39 (d, 1H, $J = 16.0$ Hz), 7.20 (dd, 1H, $J = 2.0, 8.5$ Hz), 7.15 (d, 1H, $J = 2.0$ Hz), 6.98 (d, 2H, $J = 9.0$ Hz), 6.92 (d, 1H, $J = 8.0$ Hz), 4.12 (t, 2H, $J = 7.0$ Hz), 3.92 (s, 3H), 3.88 (s, 3H), 2.51 (t, 2H, $J = 7.0$ Hz), 2.46–2.39 (m, 4H), 2.10–2.04 (m, 2H), 1.94–1.87 (m, 4H), 1.64–1.56 (m, 2H); ^{13}C NMR (125 MHz, CDCl_3): δ 189.3, 151.3, 149.6, 145.7, 138.9, 136.8, 129.9 (2C), 128.9 (2C), 127.5, 123.3, 119.3, 112.4, 110.6, 68.8, 59.0, 56.1, 54.6 (2C), 27.2, 25.9 (2C), 24.4, 23.4; HRMS (ESI); m/z calcd. for $\text{C}_{25}\text{H}_{31}\text{NO}_4$, 410.2331, found 410.2326 $[\text{M} + \text{H}]^+$.

4.2.2. (*E*)-1-(2-Hydroxyphenyl)-3-(3-methoxy-4-(3-(piperidin-1-yl)propoxy)phenyl)prop-2-en-1-one (**4b**). Yellowish brown liquid, yield 88%; ^1H NMR (500 MHz, CDCl_3): δ 12.94 (s, 1H), 7.94 (dd, 1H, $J = 1.5, 8.0$ Hz), 7.88 (d, 1H, $J = 15.0$ Hz), 7.53–7.48 (m, 2H), 7.25 (dd, 1H, $J = 1.9, 8.3$ Hz), 7.17 (d, 1H, $J = 2.0$ Hz), 7.03 (dd, 1H, $J = 1.0, 8.5$ Hz), 6.96–6.93 (m, 2H), 4.14 (t, 2H, $J = 7.0$ Hz), 3.94 (s, 3H), 2.49 (t, 2H, $J = 7.0$ Hz), 2.45–2.37 (m, 4H), 2.08–2.03 (m, 2H), 1.61–1.57 (m, 4H), 1.50–1.41 (m, 2H); ^{13}C NMR (125 MHz, CDCl_3): δ 189.5, 151.3, 149.6, 145.7, 137.3,

131.9 (2C), 130.0 (2C), 129.7, 127.5, 123.3, 119.3, 112.6, 110.7, 67.6, 56.1, 55.7, 54.5 (2C), 26.5, 25.9 (2C), 24.4; HRMS (ESI): m/z calcd. for $C_{24}H_{30}NO_4$, 396.2175, found 396.2165 [M + H]⁺.

4.2.3. (*E*)-1-(4-Bromophenyl)-3-(3-methoxy-4-(3-(piperidin-1-yl)propoxy)phenyl)prop-2-en-1-one (**4c**). Yellow liquid, yield 80%; ¹H NMR (500 MHz, CDCl₃): δ 7.88 (d, 1H, J = 8.5 Hz), 7.80 (d, 1H, J = 8.5 Hz), 7.76 (d, 1H, J = 15.5 Hz), 7.64 (d, 1H, J = 8.5 Hz), 7.58 (d, 1H, J = 8.5 Hz), 7.32 (d, 1H, J = 15.5 Hz), 7.21 (dd, 1H, J = 2.0, 8.5 Hz), 7.14 (d, 1H, J = 2 Hz), 6.93 (d, 1H, J = 8.5 Hz), 4.13 (t, 2H, J = 6.5 Hz), 3.92 (s, 3H), 2.50 (t, 2H, J = 7.5 Hz), 2.43–2.37 (m, 4H), 2.09–2.01 (m, 4H), 1.62–1.57 (m, 4H); ¹³C NMR (125 MHz, CDCl₃): δ 189.5, 151.3, 149.6, 145.7, 137.3, 131.9 (2C), 130.0 (2C), 129.7, 127.6, 123.3, 119.3, 112.6, 110.7, 67.6, 56.1, 55.7, 54.6 (2C), 26.5, 25.9 (2C), 24.4; HRMS (ESI): m/z calcd. for $C_{24}H_{28}BrNO_3$, 458.1331, found 458.1327 [M + H]⁺.

4.2.4. (*E*)-3-(3-Methoxy-4-(4-(piperidin-1-yl)butoxy)phenyl)-1-phenylprop-2-en-1-one (**4d**). Brown semi-solid; ¹H NMR (500 MHz, CDCl₃): δ 8.02 (dd, 2H, J = 5.0, 3.2 Hz), 7.78 (d, 1H, J = 15.6 Hz), 7.61–7.58 (m, 1H), 7.52 (t, 2H, J = 7.8 Hz), 7.40 (d, 1H, J = 15.1 Hz), 7.25–7.22 (dd, 1H, J = 1.9, 8.3 Hz), 7.18 (d, 1H, J = 1.9 Hz), 6.91 (d, 1H, J = 2.0 Hz), 4.11 (t, 2H, J = 6.7 Hz), 3.94 (s, 3H), 2.48–2.36 (m, 6H), 1.94–1.82 (m, 2H), 1.75–1.68 (m, 2H), 1.64–1.59 (m, 4H), 1.48–1.42 (m, 2H); ¹³C NMR (125 MHz, CDCl₃): δ 190.7, 151.1, 149.6, 145.2, 138.5, 132.5, 128.6 (2C), 128.4 (2C), 127.7, 123.2, 120.0, 112.4, 110.6, 68.8, 58.9, 56.1, 54.6 (2C), 27.2, 25.9 (2C), 24.4, 23.3; HRMS (ESI) calcd. for $C_{25}H_{32}NO_3$, 394.2382, found 394.2388 [M + H]⁺.

4.2.5. (*E*)-1-(4-Bromophenyl)-3-(3-methoxy-4-(4-(piperidin-1-yl)butoxy)phenyl)prop-2-en-1-one (**4e**). Brown semi-solid; ¹H NMR (500 MHz, CDCl₃): δ 8.12 (t, J = 1.7 Hz, 1H), 8.12 (t, J = 1.6 Hz, 1H), 7.92 (d, J = 7.8 Hz, 1H), 7.77 (d, J = 15.5 Hz, 1H), 7.38 (t, J = 7.8 Hz, 1H), 7.34–7.31 (m, 1H), 7.15 (d, J = 1.9 Hz, 1H), 6.90 (d, J = 8.3 Hz, 1H), 6.77 (d, J = 2.0 Hz, 1H), 4.09 (t, J = 6.7 Hz, 2H), 3.94 (s, 3H), 2.43–2.36 (m, 6H), 1.90–1.83 (m, 2H), 1.63–1.57 (m, 4H), 1.48–1.41 (m, 2H); ¹³C NMR (125 MHz, CDCl₃): δ 189.1, 151.3, 149.6, 146.1, 140.4, 136.0, 135.4, 131.2, 130.2, 126.9, 126.6, 123.5, 119.2, 112.4, 110.6, 68.8, 58.9, 56.1, 54.5 (2C), 27.2, 25.8 (2C), 24.4, 23.3; HRMS (ESI) calcd. for $C_{25}H_{31}BrNO_3$, 472.1487, found 472.1486 [M + H]⁺.

4.2.6. (*E*)-1-(4-Chlorophenyl)-3-(3-methoxy-4-(4-(piperidin-1-yl)butoxy)phenyl)prop-2-en-1-one (**4f**). Yellow solid; Mp: 79–80 °C; ¹H NMR (500 MHz, CDCl₃): δ 7.95 (d, 2H, *J* = 6.8 Hz), 7.76 (d, 1H, *J* = 15.6 Hz), 7.47 (d, 2H, *J* = 5.6 Hz), 7.33 (d, 1H, *J* = 15.6 Hz), 7.21 (dd, 1H, *J* = 8.3, 1.8 Hz), 7.15 (s, 1H), 6.90 (d, 1H, *J* = 7.4 Hz), 4.09 (t, 2H, *J* = 6.7 Hz), 3.93 (s, 3H), 2.51–2.27 (m, 7H), 1.95–1.85 (m, 2H), 1.74–1.64 (m, 2H), 1.64–1.51 (m, 4H), 1.47–1.40 (m, 2H); ¹³C NMR (125 MHz, CDCl₃): δ 189.3, 151.2, 149.6, 145.7, 138.9, 136.8, 129.8 (2C), 128.9 (2C), 127.5, 123.3, 119.3, 112.4, 110.6, 68.8, 58.9, 56.0, 54.6 (2C), 27.2, 25.9 (2C), 24.4, 23.4; HRMS (ESI) calcd. for C₂₅H₃₁ClNO₃, 428.1992, found 428.1990 [M + H]⁺.

4.2.7. (*E*)-1-(2,4-Dichlorophenyl)-3-(3-methoxy-4-(4-(piperidin-1-yl)butoxy)phenyl)prop-2-en-1-one (**4g**). Yellow solid; Mp: 79–80 °C; ¹H NMR (500 MHz, CDCl₃): δ 7.48 (d, 1H, *J* = 1.9 Hz), 7.42–7.33 (m, 3H), 7.12 (dd, 1H, *J* = 8.8, 1.9 Hz), 7.07 (d, 1H, *J* = 1.9 Hz), 6.96 (d, 1H, *J* = 15.9 Hz), 6.88 (d, 1H, *J* = 8.4 Hz), 4.08 (t, 2H, *J* = 6.7 Hz), 3.89 (s, 3H), 2.48–2.37 (m, 6H), 1.92–1.83 (m, 2H), 1.72–1.66 (m, 2H), 1.64–1.57 (m, 4H), 1.47–1.42 (m, 2H); ¹³C NMR (125 MHz, CDCl₃): δ 192.8, 151.5, 149.6, 147.1, 137.7, 136.6, 132.3, 130.2, 130.1, 127.2, 127.0, 123.9, 123.6, 112.4, 110.5, 68.8, 58.8, 56.0, 54.5 (2C), 27.1, 25.7 (2C), 24.3, 23.2; HRMS (ESI) calcd for C₂₅H₃₀Cl₂NO₃, 462.1603, found 462.1618 [M + H]⁺.

4.2.8. (*E*)-3-(3-Methoxy-4-(2-morpholinoethoxy)phenyl)-1-(4-methoxyphenyl)prop-2-en-1-one (**4h**). Yellow liquid, yield 78%; ¹H NMR (500 MHz, CDCl₃): δ 8.06–8.00 (m, 2H), 7.75 (d, 1H, *J* = 15.5 Hz), 7.41 (d, 1H, *J* = 15.5 Hz), 7.21 (dd, 1H, *J* = 2.0 Hz, 9.0 Hz), 7.16 (d, 1H, *J* = 2.0 Hz), 7.01–6.96 (m, 2H), 6.91 (d, 1H, *J* = 8.3 Hz), 4.20 (t, 2H, *J* = 6.0 Hz), 3.92 (s, 3H), 3.89 (s, 3H), 3.75–3.73 (m, 4H), 2.86 (t, 2H, *J* = 6.0 Hz), 2.61–2.59 (m, 4H); ¹³C NMR (125 MHz, CDCl₃): δ 188.7, 163.2, 150.4, 149.6, 144.0, 131.2, 130.7 (2C), 128.4, 122.7, 119.9, 113.7 (2C), 112.8, 110.7, 66.8 (2C), 66.6, 57.3, 56.0, 55.4, 54.0 (2C); HRMS (ESI): *m/z* calcd. for C₂₃H₂₈NO₅, 398.1967, found 398.1969 [M + H]⁺.

4.2.9. (*E*)-1-(4-Bromophenyl)-3-(3-methoxy-4-(2-morpholinoethoxy)phenyl)prop-2-en-1-one (**4i**). Yellow liquid, yield 83%; ¹H NMR (500 MHz, CDCl₃): δ 7.89–7.85 (m, 1H), 7.80 (d, 1H, *J* = 8.5 Hz), 7.76 (d, 1H, *J* = 15.5 Hz), 7.66–7.63 (m, 1H), 7.59 (d, 1H, *J* = 9.0 Hz), 7.33 (d, 1H, *J* = 15.5 Hz), 7.21 (dd, 1H, *J* = 2.0 Hz, 8.0 Hz), 7.15 (d, 1H, *J* = 2.0 Hz), 6.91 (d, 1H, *J* = 8.5 Hz), 4.21 (t, 2H, *J* = 6.0 Hz), 3.92 (s, 3H), 3.75–3.72 (m, 4H), 2.87 (t, 2H, *J* = 6.0 Hz), 2.61–2.59 (m,

4H); ^{13}C NMR (125 MHz, CDCl_3): δ 188.8, 163.3, 150.4, 149.6, 144.0, 131.3, 130.7 (2C), 128.5, 122.8, 120.0, 113.8 (2C), 113.0, 110.8, 66.8, 66.6, 57.3, 56.0, 55.5, 54.0 (2C); HRMS (ESI): m/z calcd. for $\text{C}_{22}\text{H}_{25}\text{BrNO}_4$, 446.0967, found 446.0960 $[\text{M} + \text{H}]^+$.

4.2.10. (*E*)-1-(2,4-Dichlorophenyl)-3-(3-methoxy-4-(2-morpholinoethoxy)phenyl)prop-2-en-1-one (**4j**). Yellow liquid, yield 86%; ^1H NMR (CDCl_3 , 500 MHz): δ 7.48 (d, 1H, $J = 2.0$ Hz), 7.41 (d, 1H, $J = 8.0$ Hz), 7.38–7.34 (m, 2H), 7.13 (dd, 1H, $J = 2.0, 8.5$ Hz), 7.07 (d, 1H, $J = 2.0$ Hz), 6.96 (d, 1H, $J = 16.0$ Hz), 6.89 (d, 1H, $J = 8.0$ Hz), 4.19 (t, 2H, $J = 6.0$ Hz), 3.89 (s, 3H), 3.74–3.72 (m, 4H), 2.86 (t, 2H, $J = 6.0$ Hz), 2.60–2.58 (m, 2H); ^{13}C NMR (125 MHz, CDCl_3): δ 192.7, 151.1, 149.7, 146.8, 137.7, 136.7, 132.2, 130.2, 130.1, 127.5, 127.2, 124.1, 123.4, 112.8, 110.6, 66.9 (2C), 66.8, 57.3, 56.0, 54.1 (2C); HRMS (ESI): m/z calcd. for $\text{C}_{22}\text{H}_{24}\text{Cl}_2\text{NO}_4$, 436.1082, found 436.1078 $[\text{M} + \text{H}]^+$.

4.2.11. (*E*)-3-(3-Methoxy-4-(2-morpholinoethoxy)phenyl)-1-(4-(trifluoromethyl)phenyl)prop-2-en-1-one (**4k**). Yellow liquid, yield 88%; ^1H NMR (500 MHz, CDCl_3): δ 8.08 (d, 2H, $J = 8.0$ Hz), 7.79–7.74 (m, 3H), 7.33 (d, 1H, $J = 16.0$ Hz), 7.22 (d, 1H, $J = 6.5$ Hz), 7.15 (s, 1H), 6.92 (d, 1H, $J = 8.0$ Hz), 4.21 (t, 2H, $J = 6.0$ Hz), 3.93 (s, 3H), 3.74–3.71 (m, 4H), 2.89–2.84 (m, 2H), 2.62–2.59 (m, 4H); ^{13}C NMR (125 MHz, CDCl_3): δ 189.8, 151.0, 149.7, 146.2, 141.4, 128.7 (2C), 128.6, 128.5, 127.9, 125.8, 125.7, 125.6, 125.6, 123.3, 119.7, 112.9, 110.7, 66.8 (2C), 66.6, 57.3, 56.1, 54.0 (2C); HRMS (ESI): m/z calcd. for $\text{C}_{23}\text{H}_{25}\text{F}_3\text{NO}_4$, 436.1736, found 436.1727 $[\text{M} + \text{H}]^+$.

4.2.12. (*E*)-3-(3-Methoxy-4-(3-morpholinopropoxy)phenyl)-1-(4-methoxyphenyl)prop-2-en-1-one (**4l**). Yellow liquid, yield 75%; ^1H NMR (500 MHz, CDCl_3): δ 8.04 (d, 2H, $J = 7.5$ Hz), 7.74 (d, 1H, $J = 15.0$ Hz), 7.40 (d, 1H, $J = 15.0$ Hz), 7.20 (d, 1H, $J = 8.0$ Hz), 7.16 (s, 1H), 6.98 (d, 2H, $J = 11.0$ Hz), 6.91 (d, 1H, $J = 5.5$ Hz), 4.14 (t, 2H, $J = 5.5$ Hz), 3.93 (s, 3H), 3.89 (s, 3H), 3.77–3.72 (m, 4H), 2.58 (t, 2H, $J = 6.5$ Hz), 2.55–2.50 (m, 4H), 2.08–2.01 (m, 2H); ^{13}C NMR (125 MHz, CDCl_3): δ 188.8, 163.3, 150.7, 149.5, 144.3, 131.3, 130.7 (2C), 128.1, 122.9, 119.9, 113.8 (2C), 112.7, 110.8, 67.1, 66.6, 56.1, 55.5 (2C), 55.4, 53.5 (2C), 25.9; HRMS (ESI): m/z calcd for $\text{C}_{24}\text{H}_{30}\text{NO}_5$, 412.2124, found 412.2113 $[\text{M} + \text{H}]^+$.

4.2.13. (*E*)-3-(4-(3-(2,6-Dimethylmorpholino)propoxy)-3-methoxyphenyl)-1-(4-methoxyphenyl)prop-2-en-1-one (**4m**). Yellow semi-solid, yield 85%; ^1H NMR (500 MHz, CDCl_3): δ 8.03 (d, 2H, $J = 6.5$ Hz), 7.75 (d, 1H, $J = 15.5$ Hz), 7.40 (d, 1H, $J = 15.5$ Hz), 7.20 (d, 1H, $J = 8.0$ Hz), 7.16 (s, 1H), 6.97 (d, 2H, $J = 8.5$ Hz), 6.91 (d, 1H, $J = 8.0$ Hz), 4.13 (t, 2H, $J = 6.5$ Hz), 3.92 (s, 3H), 3.88 (s, 3H), 3.70–3.65 (m, 2H), 2.76 (d, 2H, $J = 11.0$ Hz), 2.51 (t, 2H, $J = 7.0$ Hz), 2.08–2.02 (m, 2H), 1.74 (t, 2H, $J = 11.0$ Hz), 1.16 (s, 3H), 1.15 (s, 3H); ^{13}C NMR (125 MHz, CDCl_3): δ 188.7, 163.2, 150.7, 149.5, 144.1, 131.2, 130.6 (2C), 128.0, 122.8, 119.7, 113.7 (2C), 112.5, 110.6, 71.5 (2C), 67.2, 59.4 (2C), 56.0, 55.4, 54.8, 26.1, 19.1 (2C); HRMS (ESI): m/z calcd. for $\text{C}_{26}\text{H}_{34}\text{NO}_5$, 440.2437, found 440.2457 $[\text{M} + \text{H}]^+$.

4.2.14. (*E*)-3-(4-(3-(2,6-Dimethylmorpholino)propoxy)-3-methoxyphenyl)-1-(2-methoxyphenyl)prop-2-en-1-one (**4n**). Yellow semi-solid, yield 80%; ^1H NMR (500 MHz, CDCl_3): δ 7.93 (d, 2H, $J = 8.0$ Hz), 7.75 (d, 1H, $J = 15.5$ Hz), 7.38 (d, 1H, $J = 15.5$ Hz), 7.30 (d, 2H, $J = 8.5$ Hz), 7.20 (d, 1H, $J = 8.5$ Hz), 7.16 (s, 1H), 6.91 (d, 1H, $J = 8.5$ Hz), 4.13 (t, 2H, $J = 6.5$ Hz), 3.93 (s, 3H), 3.70–3.65 (m, 2H), 2.76 (d, 2H, $J = 12.0$ Hz), 2.51 (t, 2H, $J = 7.0$ Hz), 2.44 (s, 3H), 2.07–2.00 (m, 2H), 1.74 (t, 2H, $J = 11.0$ Hz), 1.17 (s, 3H), 1.15 (s, 3H); ^{13}C NMR (125 MHz, CDCl_3): δ 190.1, 150.8, 149.5, 144.6, 143.4, 135.9, 129.2 (2C), 128.6 (2C), 127.9, 123.0, 120.0, 112.6, 110.6, 71.6 (2C), 67.2, 59.4 (2C), 56.0, 54.9, 26.1, 21.6, 19.1 (2C); HRMS (ESI): m/z calcd. for $\text{C}_{26}\text{H}_{34}\text{NO}_5$, 440.2437, found 440.2432 $[\text{M} + \text{H}]^+$.

4.2.15. (*E*)-1-(2,4-Dichlorophenyl)-3-(4-(3-(2,6-dimethylmorpholino)propoxy)-3-methoxyphenyl)prop-2-en-1-one (**4o**). Yellow solid, yield 78%; Mp: 98–100 °C; ^1H NMR (500 MHz, CDCl_3): δ 7.48 (d, 1H, $J = 2.0$ Hz), 7.41 (d, 1H, $J = 8.0$ Hz), 7.38–7.33 (m, 2H), 7.11 (dd, 1H, $J = 2.0, 8.5$ Hz), 7.07 (d, 1H, $J = 2.0$ Hz), 6.96 (d, 1H, $J = 16.0$ Hz), 6.89 (d, 1H, $J = 8.5$ Hz), 4.12 (t, 2H, $J = 6.5$ Hz), 3.89 (s, 3H), 3.68–3.65 (m, 2H), 2.75 (d, 2H, $J = 10.5$ Hz), 2.49 (t, 2H, $J = 7.0$ Hz), 2.06–2.01 (m, 2H), 1.73 (t, 2H, $J = 10.5$ Hz), 1.16 (s, 3H), 1.15 (s, 3H); ^{13}C NMR (125 MHz, CDCl_3): δ 192.7, 151.4, 149.6, 147.0, 137.7, 136.6, 132.2, 130.2, 130.1, 127.2, 127.1, 123.9, 123.5, 112.5, 110.5, 71.6 (2C), 67.2, 59.5 (2C), 56.0, 54.8, 26.1, 19.1 (2C); HRMS (ESI): m/z calcd. for $\text{C}_{25}\text{H}_{30}\text{Cl}_2\text{NO}_4$, 478.1552, found 478.1547 $[\text{M} + \text{H}]^+$.

4.2.16. (*E*)-3-(4-(3-(2,6-Dimethylmorpholino)propoxy)-3-methoxyphenyl)-1-*p*-tolylprop-2-en-1-one (**4p**). Yellow semi-solid, yield 80%; ^1H NMR (500 MHz, CDCl_3): δ 7.93 (d, 2H, $J = 7.5$ Hz),

7.75 (d, 1H, $J = 15.5$ Hz), 7.39 (d, 1H, $J = 15.5$ Hz), 7.30 (d, 2H, $J = 7.5$ Hz), 7.21 (d, 1H, $J = 8.0$ Hz), 7.16 (s, 1H), 6.92 (d, 1H, $J = 8.0$ Hz), 4.13 (t, 2H, $J = 6.5$ Hz), 3.93 (s, 3H), 3.73–3.67 (m, 2H), 2.75 (d, 2H, $J = 11.0$ Hz), 2.50 (t, 2H, $J = 12.0$ Hz), 2.43 (s, 3H), 2.07–2.02 (m, 2H), 1.74 (t, 2H, $J = 11.5$ Hz), 1.17 (s, 3H), 1.15 (s, 3H); ^{13}C NMR (125 MHz, CDCl_3): δ 190.1, 150.8, 149.5, 144.6, 143.4, 135.9, 129.2 (2C), 128.6 (2C), 127.9, 123.0, 120.0, 112.6, 110.6, 71.6 (2C), 67.2, 59.5 (2C), 56.0, 54.9, 26.2, 21.6, 19.1 (2C); HRMS (ESI): m/z calcd. for $\text{C}_{26}\text{H}_{34}\text{NO}_4$, 424.2488, found 424.2477 $[\text{M} + \text{H}]^+$.

4.2.17. (*E*)-3-(4-(3-(Indolin-1-yl)propoxy)-3-methoxyphenyl)-1-(4-methoxyphenyl)prop-2-en-1-one (**4q**). Yellow solid, yield 90%; Mp: 227–229 °C; ^1H NMR (500 MHz, CDCl_3): δ 8.04 (d, 2H, $J = 9.0$ Hz), 7.76 (d, 1H, $J = 15.5$ Hz), 7.41 (d, 1H, $J = 15.5$ Hz), 7.21 (d, 1H, $J = 8.5$ Hz), 7.17 (s, 1H), 7.09–7.03 (m, 2H), 6.99 (d, 2H, $J = 8.5$ Hz), 6.91 (d, 1H, $J = 8.5$ Hz), 6.65 (t, 1H, $J = 7.5$ Hz), 6.51 (d, 1H, $J = 8.0$ Hz), 4.19 (t, 2H, $J = 6.0$ Hz), 3.96 (s, 3H), 3.90 (s, 3H), 3.37 (t, 2H, $J = 8.5$ Hz), 3.30 (t, 2H, $J = 7.0$ Hz), 2.97 (t, 2H, $J = 8.5$ Hz), 2.17 (m, 2H); ^{13}C NMR (125 MHz, CDCl_3): δ 188.8, 163.3, 152.6, 150.8, 149.6, 144.2, 131.3, 130.7 (2C), 129.9, 128.1, 127.3, 124.4, 122.9, 119.8, 117.6, 113.8 (2C), 112.7, 110.7, 106.9, 66.7, 56.1, 55.5, 53.3, 46.0, 28.6, 27.3; HRMS (ESI): m/z calcd. for $\text{C}_{28}\text{H}_{30}\text{NO}_4$, 444.2175, found 444.2193 $[\text{M} + \text{H}]^+$.

4.2.18. (*E*)-1-(2,4-Dichlorophenyl)-3-(4-(3-(indolin-1-yl)propoxy)-3-methoxyphenyl)prop-2-en-1-one (**4r**). Off-white solid, yield 89%; Mp: 92–94 °C; ^1H NMR (500 MHz, CDCl_3): δ 7.48 (d, 1H, $J = 1.5$ Hz), 7.41 (d, 1H, $J = 8.5$ Hz), 7.38–7.34 (m, 2H), 7.11–7.01 (m, 4H), 6.96 (d, 1H, $J = 16.0$ Hz), 6.88 (d, 1H, $J = 8.0$ Hz), 6.64 (t, 1H, $J = 7.0$ Hz), 6.49 (d, 1H, $J = 8.0$ Hz), 4.18 (t, 2H, $J = 6.5$ Hz), 3.92 (s, 3H), 3.35 (t, 2H, $J = 8.5$ Hz), 3.28 (t, 2H, $J = 6.5$ Hz), 2.96 (t, 2H, $J = 8.5$ Hz), 2.16 (m, 2H); ^{13}C NMR (125 MHz, CDCl_3): δ 192.7, 152.6, 151.4, 149.7, 147.1, 137.7, 136.6, 132.3, 130.3, 130.1, 130.0, 127.3, 127.2 (2C), 124.4, 124.0, 123.6, 117.6, 112.6, 110.5, 106.9, 66.7, 56.0, 53.4, 46.0, 28.6, 27.3; HRMS (ESI): m/z calcd. for $\text{C}_{27}\text{H}_{26}\text{Cl}_2\text{NO}_3$, 482.1290, found 482.1302 $[\text{M} + \text{H}]^+$.

4.2.19. (*E*)-3-(4-(3-(3,4-Dihydroquinolin-1(2H)-yl)propoxy)-3-methoxyphenyl)-1-phenylprop-2-en-1-one (**4s**). Yellow solid; Mp: 111–113 °C; ^1H NMR (500 MHz, CDCl_3): δ 8.01 (d, 2H, $J = 7.3$ Hz), 7.76 (d, 1H, $J = 15.6$ Hz), 7.58 (t, 1H, $J = 7.3$ Hz), 7.51 (t, 2H, $J = 7.5$ Hz), 7.39 (d, 1H, $J = 15.6$ Hz), 7.19 (d, 1H, $J = 7.0$ Hz), 7.18 (s, 1H), 7.00 (t, 1H, $J = 7.5$ Hz), 6.94 (d, 1H, $J = 7.1$

Hz), 6.88 (d, 1H, $J = 8.3$ Hz), 6.64 (d, 1H, $J = 8.2$ Hz), 6.55 (t, 1H, $J = 7.2$ Hz), 4.14 (t, 2H, $J = 5.9$ Hz), 3.95 (s, 3H), 3.50 (t, 2H, $J = 6.9$ Hz), 3.29 (t, 2H, $J = 4.9$ Hz), 2.75 (t, 2H, $J = 6.3$ Hz), 2.20–2.10 (m, 2H), 1.97–1.89 (m, 2H); ^{13}C NMR (125 MHz, CDCl_3): δ 190.7, 150.9, 149.7, 145.2, 145.1, 138.5, 132.6, 129.2, 128.6 (2C), 128.5 (2C), 128.0, 127.1, 123.2, 122.4, 120.1, 115.6, 112.8, 110.7, 110.6, 66.6, 56.1, 49.7, 48.0, 28.2, 26.3, 22.3; HRMS (ESI) calcd. for $\text{C}_{28}\text{H}_{30}\text{NO}_3$, 428.2226, found 428.2284 $[\text{M} + \text{H}]^+$.

4.2.20. (*E*)-3-(4-(3-(3,4-Dihydroquinolin-1(2H)-yl)propoxy)-3-methoxyphenyl)-1-(4-methoxyphenyl)prop-2-en-1-one (**4t**). Yellow solid; Mp: 91–92 °C; ^1H NMR (500 MHz, CDCl_3): δ 8.04 (d, 2H, $J = 8.7$ Hz), 7.75 (d, 1H, $J = 15.5$ Hz), 7.41 (d, 1H, $J = 15.5$ Hz), 7.20 (d, 1H, $J = 6.0$ Hz), 7.18 (s, 1H), 7.04–6.95 (m, 3H), 6.93 (d, 1H, $J = 7.2$ Hz), 6.88 (d, 1H, $J = 8.2$ Hz), 6.64 (d, 1H, $J = 8.2$ Hz), 6.55 (t, 1H, $J = 7.2$ Hz), 4.13 (t, 2H, $J = 5.7$ Hz), 3.95 (s, 3H), 3.89 (s, 3H), 3.50 (t, 2H, $J = 6.9$ Hz), 3.29 (t, 2H, $J = 4.7$ Hz), 2.75 (t, 2H, $J = 6.3$ Hz), 2.22–2.08 (m, 2H), 2.00–1.87 (m, 2H); ^{13}C NMR (125 MHz, CDCl_3): δ 188.8, 163.3, 150.7, 149.7, 145.2, 144.2, 131.4, 130.7 (2C), 129.2, 128.2, 127.1, 122.9, 122.4, 119.8, 115.6, 113.8 (2C), 112.3, 110.8, 110.7, 66.6, 56.1, 55.5, 49.7, 48.0, 28.2, 26.3, 22.3; HRMS (ESI) calcd. for $\text{C}_{29}\text{H}_{32}\text{NO}_4$, 458.2331, found 458.2328 $[\text{M} + \text{H}]^+$.

4.2.21. (*E*)-1-(4-Bromophenyl)-3-(4-(3-(3,4-dihydroquinolin-1(2H)-yl)propoxy)-3-methoxyphenyl)prop-2-en-1-one (**4u**). Yellow solid; Mp: 95–97 °C; ^1H NMR (500 MHz, CDCl_3): δ 7.88 (d, 2H, $J = 8.1$ Hz), 7.76 (d, 1H, $J = 15.6$ Hz), 7.64 (d, 2H, $J = 8.1$ Hz), 7.32 (d, 1H, $J = 8.5$ Hz), 7.20 (d, 1H, $J = 7.3$ Hz), 7.17 (s, 1H), 7.00 (t, 1H, $J = 7.7$ Hz), 6.94 (d, 1H, $J = 7.3$ Hz), 6.88 (d, 1H, $J = 8.3$ Hz), 6.64 (d, 1H, $J = 8.2$ Hz), 6.56 (t, 1H, $J = 7.3$ Hz), 4.14 (t, 2H, $J = 6.0$ Hz), 3.95 (s, 3H), 3.50 (t, 2H, $J = 6.9$ Hz), 3.29 (t, 2H, $J = 4.9$ Hz), 2.75 (t, 2H, $J = 6.3$ Hz), 2.20–2.09 (m, 2H), 1.97–1.88 (m, 2H); ^{13}C NMR (125 MHz, CDCl_3): δ 189.5, 151.1, 149.7, 145.7, 145.2, 137.2, 131.9 (2C), 130.0 (2C), 129.2, 127.8, 127.6, 127.1, 123.3, 122.4, 119.4, 115.7, 112.7, 110.8, 110.7, 66.6, 56.1, 49.7, 48.0, 28.2, 26.3, 22.2; HRMS (ESI) calcd. for $\text{C}_{28}\text{H}_{29}\text{BrNO}_3$, 506.1331, found 506.1328 $[\text{M} + \text{H}]^+$.

4.2.22. (*E*)-1-(4-Chlorophenyl)-3-(4-(3-(3,4-dihydroquinolin-1(2H)-yl)propoxy)-3-methoxyphenyl)prop-2-en-1-one (**4v**). Yellow solid; Mp: 103–105 °C; ^1H NMR (500 MHz, CDCl_3): δ 7.96 (d, 2H, $J = 8.3$ Hz), 7.76 (d, 1H, $J = 15.6$ Hz), 7.47 (d, 2H, $J = 8.3$ Hz), 7.34 (d,

1H, $J = 15.6$ Hz), 7.20 (d, 1H, $J = 8.3$ Hz), 7.17 (s, 1H), 7.00 (t, 1H, $J = 7.7$ Hz), 6.94 (d, 1H, $J = 7.3$ Hz), 6.88 (d, 1H, $J = 8.3$ Hz), 6.63 (d, 1H, $J = 8.2$ Hz), 6.55 (t, 1H, $J = 7.3$ Hz), 4.14 (t, 2H, $J = 6.0$ Hz), 3.95 (s, 3H), 3.50 (t, 2H, $J = 6.9$ Hz), 3.28 (t, 2H, $J = 5.5$ Hz), 2.75 (t, 2H, $J = 6.2$ Hz), 2.21–2.08 (m, 2H), 2.05–1.83 (m, 2H); ^{13}C NMR (125 MHz, CDCl_3): δ 189.3, 151.1, 149.7, 145.6, 145.2, 139.0, 136.8, 129.9 (2C), 129.2, 128.9 (2C), 127.8, 127.1, 123.3, 122.4, 119.4, 115.7, 112.7, 110.8, 110.7, 66.6, 56.1, 49.7, 48.0, 28.1, 26.3, 22.3; HRMS (ESI) calcd. for $\text{C}_{28}\text{H}_{29}\text{ClNO}_3$, 462.1836, found 462.1836 [M + H] $^+$.

4.2.23. (*E*)-1-(2,4-Dichlorophenyl)-3-(4-(3-(3,4-dihydroquinolin-1(2H)-yl)propoxy)-3-methoxyphenyl)prop-2-en-1-one (**4w**). Yellow solid; Mp: 92–94 °C; ^1H NMR (500 MHz, CDCl_3): δ 7.49 (s, 1H), 7.43–7.33 (m, 3H), 7.13–7.08 (m, 2H), 7.01–6.91 (m, 3H), 6.86 (d, 1H, $J = 8.2$ Hz), 6.63 (d, 1H, $J = 8.2$ Hz), 6.55 (t, 1H, $J = 7.3$ Hz), 4.13 (t, 2H, $J = 6.0$ Hz), 3.92 (s, 3H), 3.49 (t, 2H, $J = 6.9$ Hz), 3.28 (t, 2H, $J = 5.5$ Hz), 2.74 (t, 2H, $J = 6.3$ Hz), 2.19–2.09 (m, 2H), 1.97–1.88 (m, 2H); ^{13}C NMR (125 MHz, CDCl_3): δ 188.0, 146.6, 145.0, 142.3, 140.7, 140.2, 133.0, 131.9, 127.5, 125.5, 125.4, 124.5, 122.5, 122.4, 119.3, 118.8, 117.7, 110.9, 107.9, 105.9, 61.9, 51.3, 45.0, 43.2, 23.4, 21.6, 17.5; HRMS (ESI) calcd. for $\text{C}_{28}\text{H}_{28}\text{Cl}_2\text{NO}_3$, 496.1446, found 496.1446 [M + H] $^+$.

4.2.24. (*E*)-1-(4-Aminophenyl)-3-(4-(3-(3,4-dihydroquinolin-1(2H)-yl)propoxy)-3-methoxyphenyl)prop-2-en-1-one (**4x**). Brown semi-solid; ^1H NMR (500 MHz, CDCl_3): δ 7.93 (d, 2H, $J = 8.6$ Hz), 7.73 (d, 1H, $J = 15.5$ Hz), 7.41 (d, 1H, $J = 15.5$ Hz), 7.21–7.14 (m, 2H), 7.00 (t, 1H, $J = 7.7$ Hz), 6.94 (d, 1H, $J = 7.1$ Hz), 6.87 (d, 1H, $J = 8.2$ Hz), 6.70 (d, 2H, $J = 8.5$ Hz), 6.64 (d, 1H, $J = 8.2$ Hz), 6.55 (t, 1H, $J = 7.3$ Hz), 4.13 (t, 2H, $J = 6.1$ Hz), 3.94 (s, 3H), 3.50 (t, 2H, $J = 6.9$ Hz), 3.29 (t, 2H, $J = 5.6$ Hz), 2.75 (t, 2H, $J = 6.3$ Hz), 2.22–2.04 (m, 2H), 1.97–1.85 (m, 2H), 1.67 (brs, 2H); ^{13}C NMR (125 MHz, CDCl_3): δ 183.5, 146.3, 145.8, 144.9, 140.5, 138.6, 126.3 (2C), 124.4, 124.0, 123.7, 122.4, 118.0, 117.6, 115.2, 110.9, 109.2 (2C), 108.1, 106.0, 105.9, 61.9, 51.4, 45.0, 43.3, 23.4, 21.6, 17.5; HRMS (ESI) calcd. for $\text{C}_{28}\text{H}_{31}\text{N}_2\text{O}_3$, 443.2335, found 443.2333 [M + H] $^+$.

4.2.25. (*E*)-3-(4-(3-(3,5-Dimethyl-1H-pyrazol-1-yl)propoxy)-3-methoxyphenyl)-1-(4-methoxyphenyl)prop-2-en-1-one (**4y**). Yellow semi-solid, yield 80%; ^1H NMR (500 MHz, CDCl_3): δ 8.03 (d, 2H, $J = 9.0$ Hz), 7.73 (d, 1H, $J = 15.5$ Hz), 7.39 (d, 1H, $J = 15.5$ Hz), 7.19 (dd, 1H, $J = 1.7$,

10.0 Hz), 7.15 (d, 1H, $J = 1.6$ Hz), 6.98 (d, 2H, $J = 8.5$ Hz), 6.83 (d, 1H, $J = 8.0$ Hz), 5.75 (s, 1H), 4.19 (t, 2H, $J = 6.5$ Hz), 3.98 (t, 2H, $J = 6.0$ Hz), 3.93 (s, 3H), 3.89 (s, 3H), 2.37–2.32 (m, 2H), 2.21 (s, 3H), 2.18 (s, 3H); ^{13}C NMR (125 MHz, CDCl_3): δ 188.8, 163.3, 150.4, 149.5, 147.6, 144.1, 139.2, 131.3, 130.7 (2C), 128.2, 122.8, 119.9, 113.8 (2C), 112.7, 110.6, 104.7, 65.4, 55.9, 55.5, 44.6, 29.6, 13.5, 10.7; HRMS (ESI): m/z calcd. for $\text{C}_{25}\text{H}_{29}\text{N}_2\text{O}_4$, 421.2127, found 421.2120 $[\text{M} + \text{H}]^+$.

4.3. Biology

4.3.1. Cell cultures

Cells were procured from National Centre for Cell Science (NCCS) Pune, India and stocks were maintained in the sterile laboratory conditions. Lung (A549 and NCI-H460), prostate (DU-145 and PC-3), colon (HCT-15 and HCT-116) and brain (U-87 glioblastoma) cancer cells were grown in tissue culture flasks in DMEM (Dulbecco modified Eagle medium, Sigma) or MEM (Minimum Essential Medium, Sigma) supplemented with 10% fetal bovine serum with 1X stabilized antibiotic-antimycotic solution (Sigma) in a CO_2 incubator at 37°C with 5% CO_2 and 90% relative humidity.

4.3.2. MTT assay

The cytotoxic activity of **4a–y** was determined using MTT assay. 1×10^4 cells per well were seeded in 100 μL DMEM, supplemented with 10% FBS in each well of 96-well microculture plates and incubated for 48 h, at 37°C in a CO_2 incubator. Compounds, diluted to the required concentrations in culture medium, were added to the wells with respective vehicle control. After 48 h of incubation, 10 μL MTT (3-(4,5-dimethylthiazol-2-yl)-2,5-diphenyl tetrazolium bromide) (5 mg/mL) was added to all the plates and incubated for 4 h. Then, the supernatant from each well was carefully decanted, formazon crystals were dissolved in 100 μL of DMSO and absorbance was recorded at 570 nm wavelength.

4.3.3. Morphological observations using phase contrast microscope

NCI-H460 cells were plated in 6 well culture plates with a density of 1×10^5 cells/mL and allowed to adhere for overnight. Cells were incubated with various concentrations of **4a**. After 48 h, cells

were observed for morphological changes and images were taken with phase contrast microscope (Nikon).

4.3.4. DAPI nucleic acid staining

To clearly examine nuclear morphological changes induced by compounds **4a** on NCI-H460 cells, DAPI nuclear staining was performed. Blue-fluorescent DAPI is a nuclear stain, which can cross intact membrane of live cells and stains the nucleus of the live cells as light blue, wherein the apoptotic cell nuclei appears as bright blue due to chromatin condensation. Thus, it was of our interest to examine nuclear fragmentation or chromatin condensation induced by compound **4a**. For this, NCI-H460 cells were stained with DAPI following the treatment with the compound **4a** and cells were observed under fluorescence microscope for nuclear morphological changes. The results indicate that the nuclear structure of untreated cells was intact while **4a** treated cells showed nuclear shrinkage, fragmented, pyknotic and horse shoe shaped nuclei (white arrow) and chromatin condensation, and these are the remarkable features of apoptosis. These findings demonstrate that these compounds could induce apoptosis in NCI-H460 cells.

4.3.5. Generation of Reactive Oxygen Species (ROS)

NCI-H460 cells were plated in 24 well plates at a density of (1×10^6 cells/mL) and allowed to adhere for overnight. Then the cells were treated with 1.25 μ M, 2.5 μ M and 5.0 μ M of active compound **4a** for 24 h. The media was replaced with culture medium containing DCFDA dye (10 μ M) and incubated for 30 min dark. The fluorescence intensity from samples was analysed by spectrofluorometer at an excitation and emission wavelength of 488 and 525 nm, respectively.

4.3.6. Flow-cytometry analysis

NCI-H460 cells (1×10^6 cells/well) in 6 well plate were treated with different 1.25, 2.5 and 5 μ M mM concentrations of the compound **4a** for 24 h and cells were collected by trypsinisation, washed with 150 mM PBS and were fixed with 70% ethanol for 30 min at 4 °C. After fixing, cells were washed with PBS and stained with 400 μ L of propidium

iodide staining buffer [PI (200 μ g), Triton X (100 μ L), DNase-free RNase A (2 mg) in 10 mL PBS] for 15 min at room temp in dark. The samples were then analyzed for propidium iodide fluorescence from 15,000 events by flow cytometry using BD Accuri C6 flowcytometer.

4.3.7. Effect on tubulin polymerization

Tubulin polymerization kit was purchased from Cytoskeleton, Inc. (BK011). To evaluate the effect of compound **4a**, fluorescence based *in vitro* tubulin polymerization assay was conducted following the manufacturer's protocol. The reaction mixture having porcine brain tissue (2 mg/mL) in 80 mM PIPES at pH 6.9, 2.0 mM MgCl₂, 0.5 mM EGTA, 1.0 mM GTP and glycerol in the presence and absence of test compound **4a** (final concentration of 10 μ M) was prepared and added to each well of 96-well plate. Tubulin polymerization was followed by a time dependent increase in fluorescence due to the incorporation of a fluorescence reporter into microtubules as polymerization proceeds. Fluorescence emission at 440 nm (excitation wavelength is 360 nm) was measured by using a Spectramax M4 Multi mode Micro plate Detection System. CA-4 was used as positive control in the assay at 3 μ M final concentration. The IC₅₀ value was calculated from the drug concentration required for inhibiting 50% of tubulin assembly compared to control.

4.3.8. Molecular docking

The crystal co-ordinates of α,β -tubulin subunits were retrieved from the protein data bank (PDB ID: 3E22). As the active site i.e., colchicine binding site of tubulin is located at the interface of the subunits, both the chains were considered for molecular modelling studies. The protein preparation tool was used for the preparation of receptor model (Schrödinger 2015-4). The tool adds missing side chains and loops and also removes water molecules with a distance of more than 5 Å. Then, restrained minimization was performed utilizing the OPLS 2005 force field to RMSD of 0.3 Å and an active site pocket of colchicine with 20 Å equally in each direction of X, Y, and Z was used for receptor grid generation. The potential ligands **4a** and **4b** were sketched by using 2D sketcher and, prepared for docking using Ligprep and a total number of 10 conformers were generated for each of the ligand. The ligands were docked into the active site of tubulin using GLIDE-XP (Extra Precision) flexible program.

Acknowledgements

SN, NPK, ND, DP and KRS are thankful to DoP, Ministry of Chemicals & Fertilizers, Govt. of India, New Delhi, for the award of NIPER fellowship. Dr. N. Shankaraiah thankful to SERB, DST, Govt. of India for the start-up grant (YSS-2015-001709).

References

1. Mandelkow E, Mandelkow EM. Microtubular structure and tubulin polymerization. *Curr. Opin. Cell Biol.* 1989;1:5–9.
2. Jordan MA, Wilson L. Microtubules and actin filaments: dynamic targets for cancer chemotherapy. *Curr. Opin. Cell Biol.* 1998;10:123–130.
3. Giannakakou P, Sackett D, Fojo T. Tubulin/microtubules: still a promising target for new chemotherapeutic agents. *J. Natl. Cancer Inst.* 2000;92:182–183.
4. (a) Biswas BB, Sen K, Choudhury GG, Bhattacharyya B. Molecular biology of tubulin: Its interaction with drugs and genomic organization. *J. Biosci.* 1984;6:431–457; (b) Shankaraiah N, Kumar NP, Amula SB, Nekkanti S, Jeengar MK, Naidu VG, Reddy TS, Kamal A. One-pot synthesis of podophyllotoxin–thiourea congeners by employing $\text{NH}_2\text{SO}_3\text{H/NaI}$: Anticancer activity, DNA topoisomerase-II inhibition, and apoptosis inducing agents. *Bioorg. Med. Chem. Lett.* 2015;25:4239–4244; (c) Kamal A, Reddy TS, Polepalli S, Shalini N, Reddy VG, Rao AS, Jain N, Shankaraiah N. Synthesis and biological evaluation of podophyllotoxin congeners as tubulin polymerization inhibitors. *Bioorg. Med. Chem.* 2014;22:5466–5475; (d) Kamal A, Suresh P, Ramaiah MJ, Reddy TS, Kapavarapu RK, Rao BN, Imthiajali S, Reddy TL, Pushpavalli SN, Shankaraiah N, Pal-Bhadra M. 4β -[4'-(1-(Aryl) ureido) benzamide] podophyllotoxins as DNA topoisomerase I and II α inhibitors and apoptosis inducing agents. *Bioorg. Med. Chem.* 2013;21:5198–5208; (e) Kamal A, Reddy TS, Polepalli S, Paidakula S, Srinivasulu V, Reddy VG, Jain N, Shankaraiah N. Synthesis and biological evaluation of 4-aza-2,3-dihydropyridophenanthrolines as tubulin polymerization inhibitors. *Bioorg. Med. Chem. Lett.* 2014;24:3356–3360; (f) Kamal A, Shankaraiah N, Prabhakar S, Reddy ChR, Markandeya N, Reddy KL, Devaiah V. Solid-phase synthesis of new pyrrolbenzodiazepine-chalcone conjugates: DNA-binding affinity and anticancer activity. *Bioorg. Med. Chem. Lett.* 2008;18:2434–2439.
5. terHaar E, Rosenkranz HS, Hamel E, Day BW. Computational and molecular modeling evaluation of the structural basis for tubulin polymerization inhibition by colchicine site agents. *Bioorg. Med. Chem.* 1996;4:1659–1671; (b) Kamal A, Reddy TS, Vishnuvardhan MVPS, Nimbarte VK, Rao AVS, Srinivasulu V, Shankaraiah N. Synthesis of 2-aryl-

- 1,2,4-oxadiazolo-benzimidazoles: Tubulin polymerization inhibitors and apoptosis inducing agents. *Bioorg. Med. Chem.* 2015;23:4608–4623.
6. Rai SS, Wolf JJ. Localization of the vinblastine-binding site on beta-tubulin. *J. Biol. Chem.* 1996;271:14707–14711.
 7. Andreu JM, Barasaoin I. The interaction of baccatin III with the taxol binding site of microtubules determined by a homogeneous assay with fluorescent taxoid. *Biochemistry* 2001;40:11975–11984.
 8. Downing KH, Nogales E. Tubulin structure: insights into microtubule properties and functions. *Curr. Opin. Struct. Biol.* 1998;8:785–791.
 9. Downing KH. Structural basis for the interaction of tubulin with proteins and drugs that affect microtubule dynamics. *Annu. Rev. Cell. Dev. Biol.* 2000;16:89–111.
 10. Sorger PK, Dobles M, Tournebize R, Hyman AA. Coupling cell division and cell death to microtubule dynamics. *Curr. Opin. Cell Biol.* 1997;9:807–814.
 11. Sahu NK, Balbhadra SS, Choudhary J, Kohli DV. Exploring pharmacological significance of chalcone scaffold: a review. *Curr. Med. Chem.* 2012;19:209–225.
 12. Ni L, Meng CQ, Sikorski JA. Recent advances in therapeutic chalcones. *Expert Opin. Ther. Pat.* 2004;14:1669–1691.
 13. Batovska DI, Todorova IT. Trends in utilization of the pharmacological potential of chalcones. *Curr. Clin. Pharmacol.* 2010;5:1–29.
 14. Dimmock JR, Elias DW, Beazely MA, Kandepu NM. Bioactivities of chalcones. *Curr. Med. Chem.* 1999;6:1125–1149.
 15. (a) Mirzaei H, Emami S. Recent advances of cytotoxic chalconoids targeting tubulin polymerization: Synthesis and biological activity. *Eur. J. Med. Chem.* 2016;121:610–639;
(b) Kamal A, Prabhakar S, Ramaiah MJ, Reddy PV, Reddy ChR, Mallareddy A, Shankaraiah N, Reddy TLN, Pushpavalli SNCVL, Bhadra M-P. Synthesis and anticancer activity of new chalcone-pyrrolobenzodiazepine conjugates linked via 1,2,3-triazole ring side-armed alkane spacers. *Eur. J. Med. Chem.* 2011;46:3820–3831.
 16. Go ML, Wu X, Liu XL. Chalcones: An Update on Cytotoxic and Chemoprotective Properties. *Curr. Med. Chem.* 2005;12:483–499.
 17. Ducki S. Antimitotic Chalcones and Related Compounds as Inhibitors of Tubulin Assembly. *Med. Chem.* 2009;9:336–347.

18. Dyrager C, Wickstrom M, Friden-Saxin M, Friberg A, Dahlen K, Wallen EA, Gullbo J, Grotli M, Luthman K. Inhibitors and promoters of tubulin polymerization: Synthesis and biological evaluation of chalcones and related dienones as potential anticancer agents. *Bioorg. Med. Chem.* 2011;19:2659–2665.
19. Ducki S, Rennison D, Woo M, Kendall A, Chabert JFD, McGown AT, Lawrence NJ. Combretastatin-like chalcones as inhibitors of microtubule polymerization. Part 1: Synthesis and biological evaluation of antivasular activity. *Bioorg. Med. Chem.* 2009;17:7698–7710.
20. Boumendjel A, Boccard J, Carrupt PA, Nicolle E, Blanc M, Geze A, Choisnard L, Wouessidjewe D, Matera EL, Dumontet C. Antimitotic and antiproliferative activities of chalcones: forward structure-activity relationship. *J. Med. Chem.* 2008;51:2307–2310.
21. (a) Shankaraiah N, Siraj KP, Nekkanti S, Srinivasulu V, Satish M, Sharma P, Senwar KR, Vishnuvardhan MVPS, Ramakrishna S, Kamal A. Synthesis, DNA-Binding Affinity and Cytotoxic Activity of New C3-Linked Chalcone- β -Carboline Hybrids. *Bioorg. Chem.* 2015;59:130–139; (b) Kumar NP, Nekkanti S, Kumari SS, Sharma P, Shankaraiah N, Design and synthesis of 1,2,3-triazolo-phenanthrene hybrids as cytotoxic agents. *Bioorg. Med. Chem. Lett.* 2017;27:2369–2376.
22. Kamal A, Srinivasulu V, Nayak VL, Sathish M, Shankaraiah N, Bagul C, Reddy NVS, Rangaraj N, Nagesh N. Design and synthesis of C3-pyrazole/chalcone linked β -carboline hybrids: Antitopoisomerase I, DNA interactive and apoptosis inducing anticancer agents. *ChemMedChem.* 2014;9:2084–2098.
23. (a) Shankaraiah N, Jadala C, Nekkanti S, Senwar KR, Nagesh N, Shrivastava S, Naidu VGM, Sathish M, Kamal A. Design and synthesis of C3-tethered 1,2,3-triazolo- β -carboline derivatives: Anticancer activity, DNA-binding ability, viscosity and molecular modeling studies. *Bioorg. Chem.* 2016;64:42–50; (b) Kumar NP, Sharma P, Reddy TS, Nekkanti S, Shankaraiah N, Lalitha G, Sujanakumari S, Bhargava SK, Naidu VGM, Kamal A. Synthesis of 2,3,6,7-tetramethoxyphenanthren-9-amine: An efficient precursor to access new 4-aza-2,3-dihydropyridophenanthrenes as apoptosis inducing agents. *Eur. J. Med. Chem.* 2017;127:305–317.
24. Shankaraiah N, Nekkanti S, Chudasama KJ, Senwar KR, Sharma P, Jeengar MK, Naidu VGM, Srinivasulu V, Kamal A. Design, Synthesis and Anticancer Evaluation of Tetrahydro- β -Carboline-hydantoin Hybrids. *Bioorg. Med. Chem. Lett.* 2014;24:5413–5417.

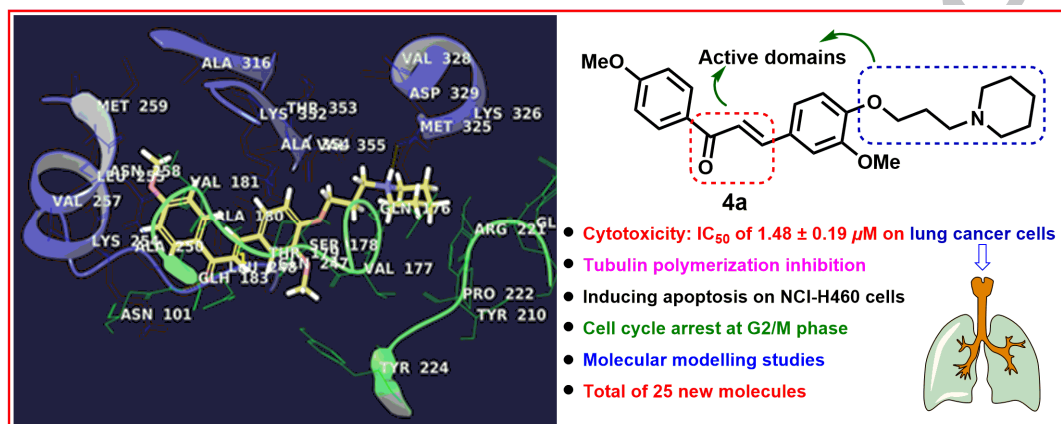
25. Nekkanti S, Veeramani K, Kumari SS, Tokala R, Shankaraiah N. A Recyclable and Water Soluble Copper(I)-Catalyst: One-pot Synthesis of 1,4-Disubstituted 1,2,3-Triazoles and their Biological Evaluation. *RSC Adv.* 2016;6:103556–103566.
26. Kennedy SG, Kandel ES, Cross TK, Hay N. Akt/Protein kinase B inhibits cell death by preventing the release of cytochrome c from mitochondria. *Mol. Cell Biol.* 1999;19:5800–5810.
27. Eruslanov E, Kusmartsev S. Identification of ROS using oxidized DCFDA and flow-cytometry. *Methods Mol Biol.* 2010;594:57–72.
28. Lawrence NJ, McGown AT, Ducki S, Hadfield JA. The interaction of chalcones with tubulin. *Anticancer Drug Des.* 2000;15:135–141.
29. Kanthou C, Greco O, Stratford A, Cook I, Knight R, Benzakour O, Tozer G. The tubulin-binding agent combretastatin A-4-phosphate arrests endothelial cells in mitosis and induces mitotic cell death. *Am. J. Pathol.* 2004;165:1401–1411.
30. Ravelli RB, Gigant B, Curmi PA, Jourdain I, Lachkar S, Sobel A, Knossow M. Insight into tubulin regulation from a complex with colchicine and a stathmin-like domain. *Nature* 2004;428:198–202.

Synthesis of different heterocycles-linked chalcone conjugates as cytotoxic agents and tubulin polymerization inhibitors

Nagula Shankaraiah,^{a*} Shalini Nekkanti,^a Uma Rani Brahma,^b Niggula Praveen Kumar,^a Namrata Deshpande,^a Daasi Prasanna,^a Kishna Ram Senwar,^a Uppu Jaya Lakshmi^b

^aDepartment of Medicinal Chemistry, National Institute of Pharmaceutical Education and Research (NIPER), Hyderabad-500 037, India

^bDepartment of Pharmacology & Toxicology, National Institute of Pharmaceutical Education and Research (NIPER), Hyderabad-500 037, India



- New heterocycles-linked chalcone conjugates were synthesized.
- Anticancer activity was tested on selected human cancer cell lines.
- The compound **4a** effectively inhibited polymerization of tubulin in a cell-free assay.
- **4a** induced apoptosis and generation of ROS on NCI-H460 cells.
- **4a** arrested on NCI-H460 cells in G2/M phase of cell cycle.

ACCEPTED MANUSCRIPT